

Primary Human Testicular Cells Self-Organize into Organoids with Testicular Properties

Yoni Baert,^{1,*} Joery De Kock,² João P. Alves-Lopes,³ Olle Söder,³ Jan-Bernd Stukenborg,^{3,4} and Ellen Goossens^{1,4}

¹Biology of the Testis, Research Laboratory for Reproduction, Genetics and Regenerative Medicine, Vrije Universiteit Brussel (VUB), 1090 Brussels, Belgium

²Department of In Vitro Toxicology and Dermato-Cosmetology, Center for Pharmaceutical Research, Vrije Universiteit Brussel (VUB), 1090 Brussels, Belgium

³Pediatric Endocrinology Unit; Q2:08, Department of Women's and Children's Health, Karolinska Institutet and University Hospital, 17176 Stockholm, Sweden

⁴Co-senior author

*Correspondence: yonibaert@vub.ac.be

<http://dx.doi.org/10.1016/j.stemcr.2016.11.012>

SUMMARY

So far, successful de novo formation of testicular tissue followed by complete spermatogenesis in vitro has been achieved only in rodents. Our findings reveal that primary human testicular cells are able to self-organize into human testicular organoids (TOs), i.e., multi-cellular tissue surrogates, either with or without support of a biological scaffold. Despite lacking testis-specific topography, these mini-tissues harbored spermatogonia and their important niche cells, which retained specific functionalities during long-term culture. These observations indicate the possibility of in vitro re-engineering of a human testicular microenvironment from primary cells. Human TOs might help in the development of a biomimetic testicular model that would exert a tremendous impact on research and development, clinical treatment of infertility, and screening in connection with drug discovery and toxicology.

INTRODUCTION

The search for an appropriate in vitro model for the testis has been ongoing for nearly a century (Martinovitch, 1937; Reda et al., 2016). In mice, classical organ culture procedures have been adapted and optimized for testicular tissue, thereby achieving complete spermatogenesis from spermatogonial stem cells (SSCs) to the formation of fertilization-competent sperm (Sato et al., 2011). However, an adequate in vitro model for human spermatogenesis has yet to be developed, despite reports of the differentiation of meiotic and post-meiotic germ cells into fertilization-competent gametes (Cremades et al., 2001).

Organoid systems take advantage of the self-organizing capabilities of cells to create diverse multi-cellular tissue surrogates that constitute a powerful novel class of biological models (Yin et al., 2016). Clearly, formation of a functional testicular organoid (TO) from a single-cell suspension would be an extremely valuable testicular model. Such de novo formation of testicular tissue, with seminiferous tubules and an interstitial compartment, has been achieved in vitro starting from isolated murine testicular somatic and germ cells without the support of a scaffold. However, in this system, spermatogenesis was arrested at the meiotic phase (Yokonishi et al., 2013). More promising results have been obtained with artificial 3D scaffolds. For example, cultivation of immature rodent testicular cells in a collagen, agarose, or methylcellulose matrix was successful in generating post-meiotic cells (Lee et al., 2006; Stukenborg et al., 2009). However, with these approaches,

specific cell orientation (normally provided by the basement membrane) is lacking, which might be responsible for its low efficiency. Notably, in a system consisting of immature rat testicular cells in a 3D agarose matrix, spermatogonia without close contact to Sertoli cells stopped developing (Reda et al., 2014).

This problem might be circumvented by using a scaffold that mimics the testicular architecture. Indeed, it is already common in tissue engineering to use scaffolds composed of biological extracellular matrix (ECM) (Brown and Badylak, 2014). In this context, we previously described the preparation of human decellularized testicular matrix (DTM) and its potential use as a scaffold (Baert et al., 2015).

Accordingly, our present goal was to re-engineer the human testicular microenvironment, including its major cellular and structural components in TOs by adding isolated suspensions of somatic and germ cells to natural testicular scaffolds. In parallel, the self-assembling capability of human testicular cells into TOs was assessed in the absence of scaffold support.

RESULTS

Formation of Scaffold-Based and Scaffold-Free TOs

To generate scaffold-based TOs, testicular cells from adult and pubertal individuals were seeded into the apical compartment of hanging transwell inserts containing 90- μ m-thick DTM (Figure 1A). In a preliminary study, we determined the thickness of DTM that was optimal for

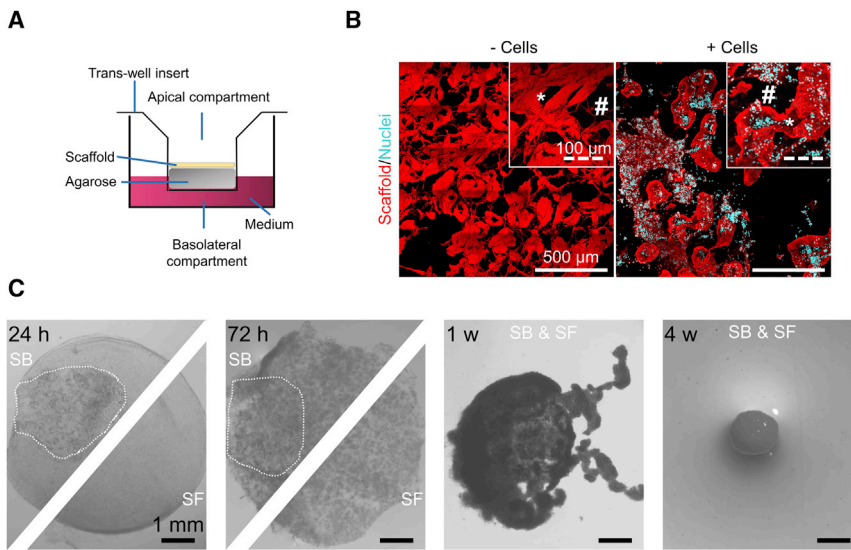


Figure 1. Formation of Scaffold-Based and Scaffold-Free TOs

(A) Schematic illustration of the culture system involving inoculation of testicular cells onto a scaffold to prepare scaffold-based (SB) TOs. Testicular cells were cultured in the apical compartment of the insert without scaffold support to form scaffold-free (SF) TOs.

(B) A testicular scaffold (red) before (left panel) and 24 hr after (right panel) cell seeding. DAPI was used to stain cell nuclei blue. The inserts show higher magnifications of a seminiferous tubule (*) and the interstitial space (#).

(C) Morphological transformation of TOs viewed through a stereomicroscope. The dotted lines delineate the re-cellularized testis scaffold. See also [Table S1](#).

cell growth with the tubules still being accessible ([Figure 1B](#), left panel). Following 24 hr of incubation, the adult or pubertal testicular cells had repopulated the scaffolds by invading the tubular structures and settling down in the interstitial compartment ([Figure 1B](#), right panel). Moreover, the cells in the scaffold were connected to the surrounding non-inoculated cells. Interestingly, with time, the testis scaffold tended to blend into the newly formed TOs. Under scaffold-free conditions, cells first self-assembled into a multi-layered cell sheet. Generally, regardless of scaffold presence, longer incubation times were associated with contraction and condensation of the TOs, finally resulting in spheroid formation after approximately 3 weeks. These spheroid structures were maintained until the end of the observation period ([Figure 1C](#)).

Spatial-Temporal Behavior of Somatic Testicular Niche Cells in TOs

In vivo, cells co-expressing the molecular steroidogenic acute regulatory protein (STAR) and steroidogenic 3 β -hydroxysteroid dehydrogenase (3 β HSD) markers are Leydig cells located in the interstitium ([Figure S1](#), top-left panel). Patches containing STAR⁺/3 β HSD⁺ cells, representing steroidogenic Leydig cells were observed for as long as 1 month in scaffold-based TOs ([Figure 2](#), top row).

In normal testicular tissue, COL1 is typically present in the interstitium, vascular wall, and tubular wall, the latter also harboring ACTA2⁺ peritubular myoid cells (PTMCs) ([Figure S1](#), middle-left panel). In the nascent TOs, randomly distributed round-shaped ACTA2⁺ cells were attached to the testicular scaffold, which stained positively for COL1. As expected, given that PTMCs are the major producers of ECM in the testis, staining for COL1 was also localized in the

cytoplasm of some ACTA2⁺ cells. Remarkably, ACTA⁻ cells were also seen to produce COL1. Later, the testis-specific pattern of COL1 distribution in TOs was replaced by a widespread network of COL1 fibers with interspersed elongated ACTA2⁺ PTMCs ([Figure 2](#), middle row), a remodeling pattern in line with our observations in stereomicroscopy. Like Leydig cells, some PTMCs in TOs appear to remain active, as indicated by this elongation and expression of ECM. Furthermore, clumps of SOX9⁺ cells expressing the tight-junction protein ZO1 were also present ([Figure 2](#), bottom row). In normal testis, SOX9⁺ Sertoli cells actively produce ZO1 as an important part of the blood-testis barrier ([Figure S1](#), bottom-left panel). These results have been reproduced in scaffold-based TOs from pubertal cells ([Figure S1](#), middle and right column). Intriguingly, similar staining patterns were also obtained in TOs formed without scaffold support ([Figure 2](#), right column). Immunostaining for immunoglobulin G (IgG) controls showed no non-specific signals and are depicted in [Figure S1](#) (fourth row).

Spatial-Temporal Behavior of Spermatogonia in TOs

Staining for each of the spermatogonial markers UCHL1, UTF1, and FGFR3 was combined with staining for the germ-cell marker DDX4 to allow unambiguous detection of early and late spermatogonia. *In situ*, these cells reside singly or aligned at the basement membrane of the seminiferous tubules ([Figure S2](#), left column). Numerous UCHL1⁺/DDX4⁺, UTF1⁺/DDX4⁺, and FGFR3⁺/DDX4⁺ cells were present in all types of TO during the 4 weeks of culture. Spermatogonia appeared as single cells and small clusters, but they also formed larger grape-like aggregates in adult TOs ([Figure 3](#), first to third row), as well as pubertal TOs ([Figure S2](#), middle and right column).

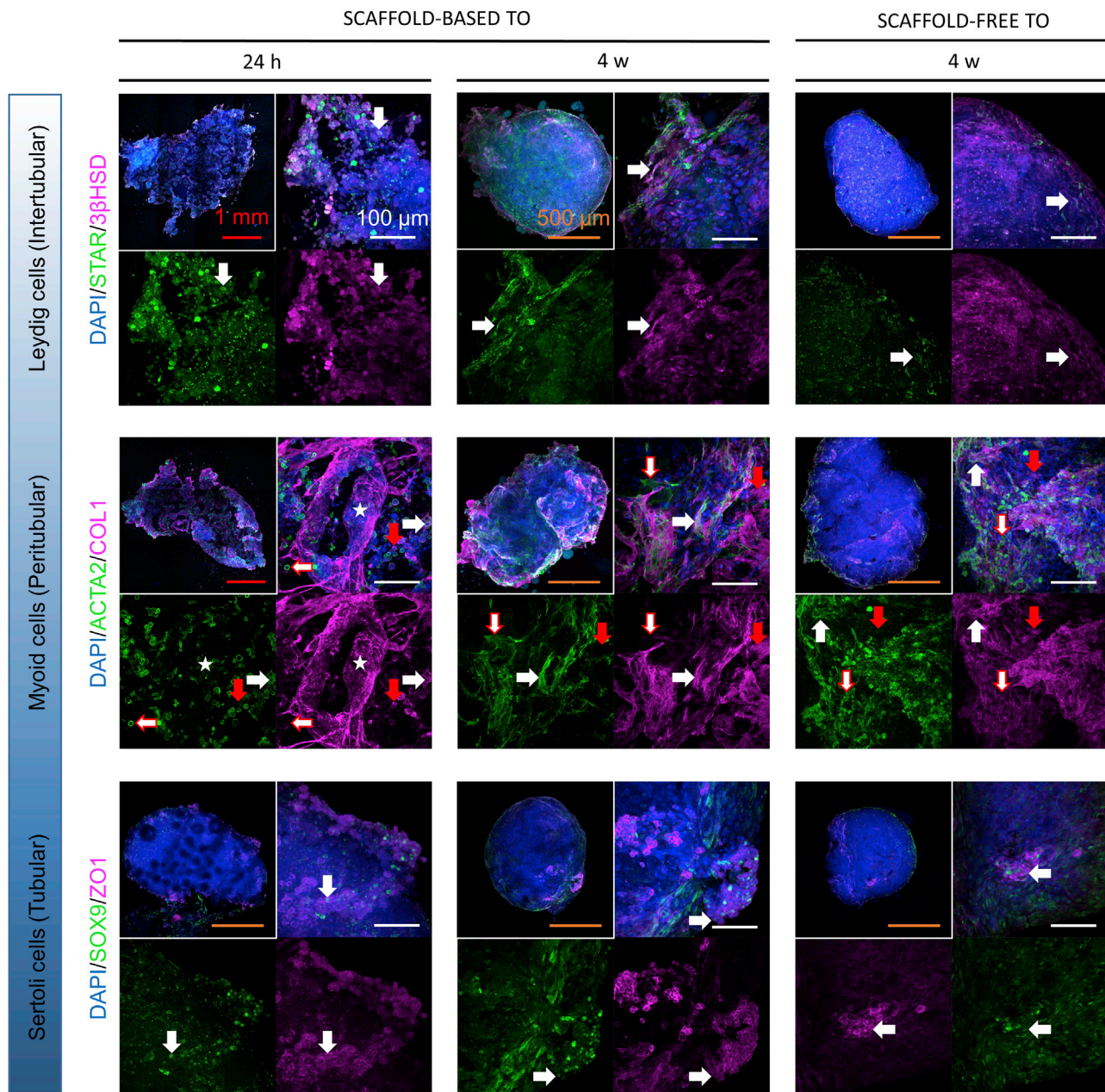
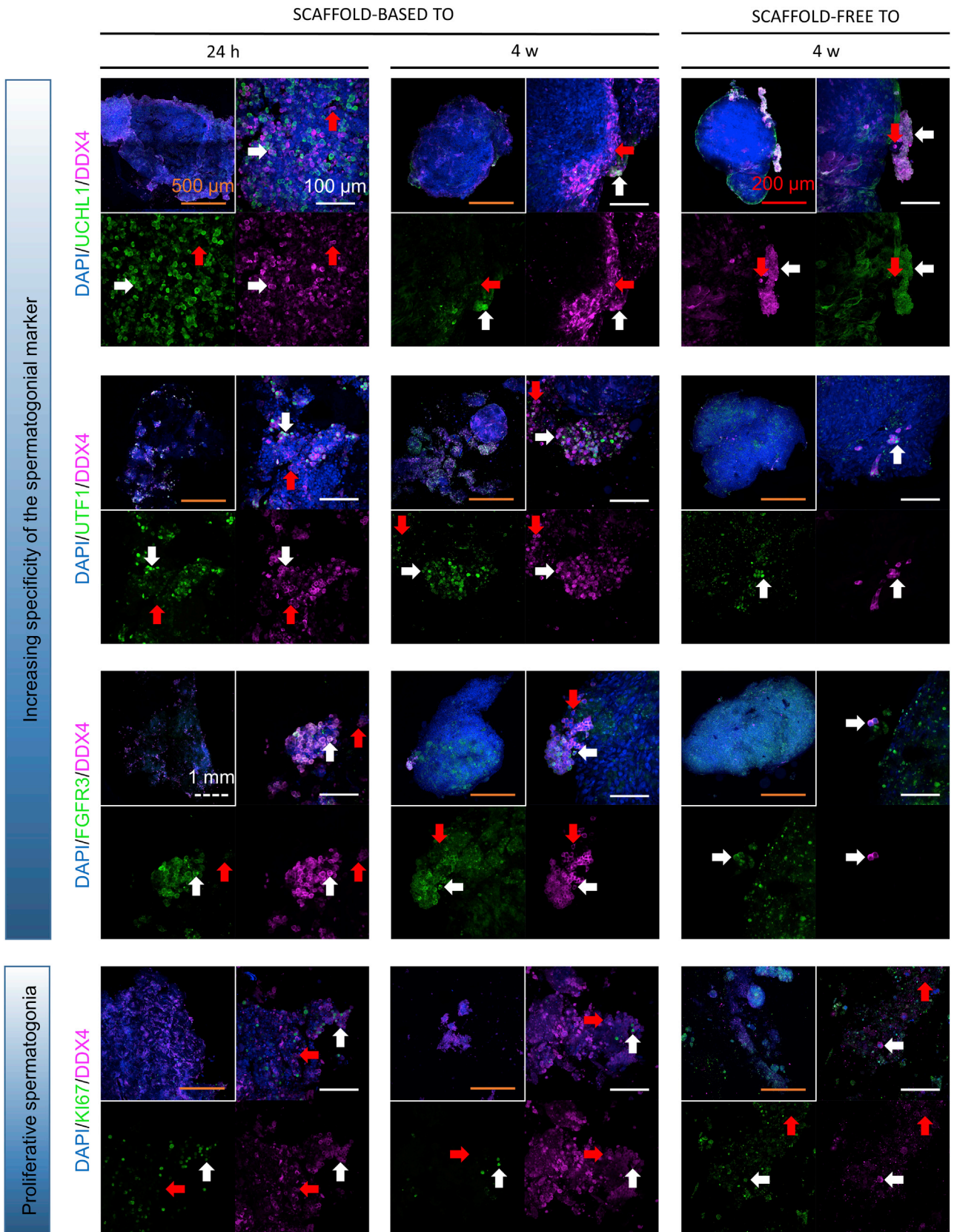


Figure 2. Characterization of Somatic Testicular Niche Cells in the TOs by Immunofluorescent Staining of Whole Mounts

Double staining for STAR/3 β HSD (top row), ACTA2/COL1 (middle row), and SOX9/ZO1 (bottom row) applied to scaffold-based (left and middle columns) and scaffold-free (right column) adult TOs ($n = 3$ TOs derived from different donors per staining). Representative photographs of TOs following short-term (left column) and long-term (middle and right columns) culture are shown. Steroidogenic Leydig cells (white arrows) stained positive for both STAR (green) and 3 β HSD (purple), PTMCs (white/red arrows) stained for ACTA2 (green), scaffold (*) and COL1-producing cells (red arrows) stained for COL1 (purple), COL1-producing PTMCs (white arrow) stained for both ACTA2 and COL1, and tight-junction protein-producing Sertoli cells (white arrow) stained for both SOX9 (green) and ZO1 (purple). Cell nuclei were stained blue with DAPI. The inserts depict several z stacks at low magnification merged with maximum intensity projection to give an overview. See also [Figure S1](#) and [Table S1](#).

Importantly, mitotically active germ cells were present in scaffold-based and scaffold-free adult TOs at both early and late time points, as revealed by expression of the protein

KI67 by DDX4⁺ cells ([Figure 3](#), fourth row). Comparable results were obtained in pubertal TOs ([Figure S2](#), second and third column). This is a crucial finding, since proliferation



(legend on next page)



is an essential functional characteristic of spermatogonia. Cells staining positive for DDX4, but not for a spermatogonial marker might be other germ-cell types that originated from the pubertal or adult donor tissue. No background staining was observed with normal rabbit or mouse IgG isotypes (Figure S1, fourth row).

Profile of Hormone and Cytokine Secretion

The maintenance of steroidogenic Leydig cells and active Sertoli cells in adult TOs was demonstrated by the detection of testosterone (T) and inhibin B (InhB), respectively, throughout the 4 weeks of culture, with comparable levels in scaffold-based and scaffold-free conditions (Figures 4A and 4B). The level of hormones produced by pubertal TOs had a tendency to increase gradually with time (Figure S3A). Strikingly, stimulation by gonadotrophins exerted no lasting effect on hormone release by Leydig and Sertoli cells in the TOs (Figures 4A, 4B, and S3A).

At 1 and 4 weeks of culture, the levels of 19 and 21 cytokines, respectively, were above threshold in the medium from at least two adult scaffold-based TOs. Scaffold-free TOs produced totals of 18 and 28 cytokines after short- and long-term culture, respectively. The majority of these cytokines were shared with scaffold-based TOs (Figures 4C and 4D). Short-term cultured scaffold-free TOs produced 14 cytokines at equal levels, while interleukin-6 (IL-6) was produced in lower amounts compared with scaffold-based TOs ($p = 0.0004$) (Figure 4C). After long-term culture, scaffold-free TOs produced GRO α ($p = 0.0349$) and IL-6 ($p < 0.0001$) at higher levels and 17 other cytokines at similar levels compared with scaffold-based TOs (Figure 4D). The cytokines restricted to scaffold-free or scaffold-based TOs are presented in Figures 4C and 4D. In addition, Figure S3B shows the cytokine secretion profiles associated with short- and long-term cultured pubertal TOs. A complete list of the cytokines assayed, including their full names is provided in Table S2 and a representative cytokine antibody array is shown in Figure S3C.

DISCUSSION

In this study, natural testis scaffolds fabricated from DTM were re-cellularized with adult and pubertal testicular cells.

Despite the fact that cells entered both the tubular and interstitial compartments, the TOs did not display typical testicular cytoarchitecture and the scaffold was remodeled by the testicular cells over time. This latter process might be initiated by breakdown of the scaffold by enzymes produced by the cells, with subsequent production of ECM proteins that re-organize the tissue.

In the light of their nature, PTMCs and Sertoli cells may have contributed directly to the reshaping of the scaffold. We show here that a number of *in vivo* testicular processes related to ECM (including the blood-testis barrier) remodeling were recapitulated in TOs derived from both young and adult cells (Díez-Torre et al., 2011; Mruk and Cheng, 2004; Siu and Cheng, 2004). First, tumor necrosis factor alpha, tissue inhibitor of metalloproteinase 1, IL-6, and monocyte chemoattractant protein 1 were produced, as detected by way of membrane antibody arrays. Second, rearrangement of COL1 fibers from a testis-specific pattern to a widespread interconnecting network occurred with time. Third, functionally differentiated PTMCs producing ECM were detected, first as round and later as elongated ACTA2⁺ cells containing COL1 in their cytoplasm and interspersed between the COL1 fibers. Fourth, co-localization of SOX9, a marker of Sertoli cells, and the tight-junction protein ZO1 in certain cells in the TOs indicated production of protein components of the blood-testis barrier by Sertoli cells. Finally, cells other than PTMCs, possibly Sertoli cells (the other main source of testicular ECM), were found to express COL1. In addition, macrophages may have played a central role as well, especially since these cells participate in the degradation of ECM scaffolds (Valentin et al., 2009). Macrophages would be expected to be present in TOs formed from suspensions containing testicular cells, given that immune cells reside naturally in the testicular interstitium (DeFalco et al., 2015). Thus, remodeling of the scaffold might have involved interactions between PTMCs, Sertoli cells, and macrophages. This phenomenon may be relevant to the observation that degradation products of ECM components, so-called cryptic peptides, regulate tissue functions (Brown and Badylak, 2014). Nevertheless, the necessity of the natural testicular scaffold in TO formation is debatable, given that the spatial-temporal behavior and hormone and cytokine secretion profiles of testicular cells in scaffold-free TOs were comparable.

Figure 3. Characterization of Spermatogonia in the TOs by Immunofluorescent Staining of Whole Mounts

Immunostaining for UCHL1/DDX4 (first row), UTF1/DDX4 (second row), FGFR3/DDX4 (third row), and KI67/DDX4 (fourth row) in adult TOs ($n = 3$ TOs derived from different donors per staining) derived with (left and middle column) and without (right column) scaffold support following 24 hr (left column) and 4 weeks (middle and right column) of culture. Representative images show cells that stained positive for UCHL1, UTF1, or FGFR3 (green), and DDX4 (purple), which are unmistakably spermatogonia (white arrow). Cells positive for DDX4 alone represent a different germ-cell type (red arrow). The DDX4⁺ (purple) cells staining for KI67 (green) are dividing germ cells (white arrow). Cell nuclei are stained blue by DAPI. The inserts depict low-magnification overviews of the TOs generated using maximum intensity projection of z stacks. See also Figure S2 and Table S1.

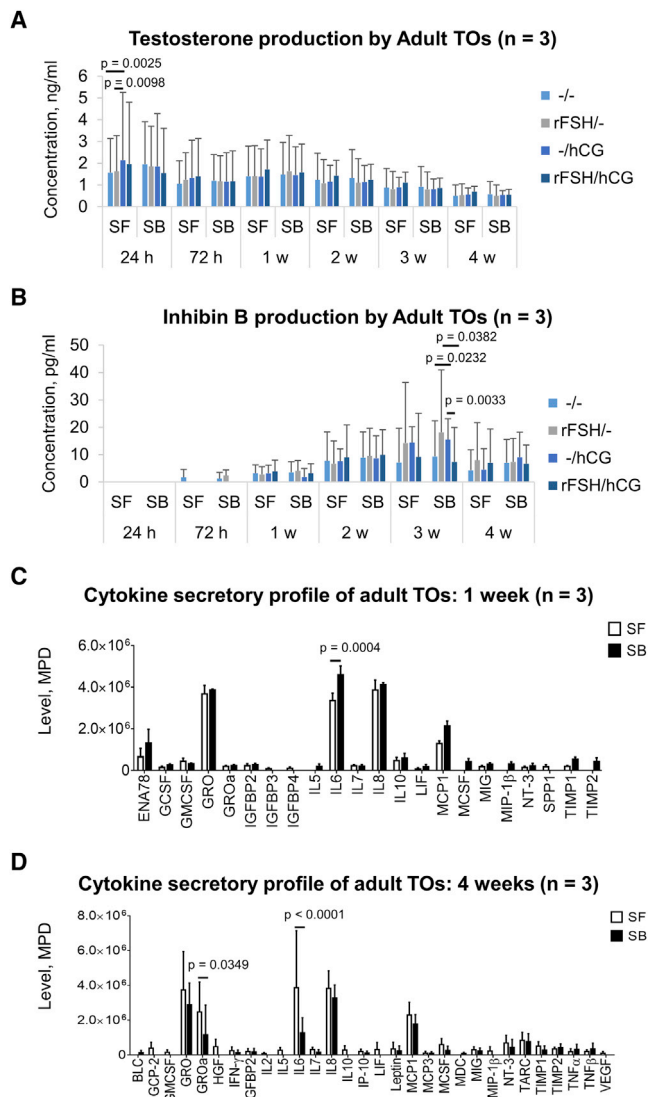


Figure 4. Secretory Profile of Hormones and Cytokines of Testicular Cells in the TOs

The levels of (A) T and (B) InhB in the medium were measured after 24 and 72 hr, and 1, 2, 3, and 4 weeks of culturing scaffold-based and scaffold-free TOs under different hormonal conditions (-/-; rFSH/-; -/hCG; rFSH/hCG). Cytokine profiles were obtained by incubating array membranes with medium from scaffold-based and scaffold-free TOs after (C) 1 week and (D) 4 weeks of culture. The data are presented as means \pm SDs (n = 3 TOs derived from different donors per condition). For an explanation of the protein abbreviations, see Table S2. hCG, human chorionic gonadotrophin; MPD, mean pixel density; rFSH, recombinant follicle-stimulating hormone; SB, scaffold based; SF, scaffold free. See also Figure S3 for the hormone and cytokine secretion profiles of pubertal TOs and a representative cytokine antibody array.

The spheroid shape of both scaffold-based and scaffold-free TOs might be explained by contraction of ACTA2 proteins in PTMCs in response to androgens, as this occurs in vivo (Schlatt et al., 1993). Importantly, we found indications of Leydig cells effecting steroidogenesis in the TOs. The presence of cells expressing STAR and 3β HSD, which are critically involved in T biosynthesis, and, in particular, the detection of T in the medium suggest Leydig cell functionality throughout the entire culture period. Interestingly, physiological concentrations of gonadotrophins did not stimulate T production, nor did they influence the production of InhB, an indicator of Sertoli cell functionality. A possible explanation for this lack of effect could be that these cells became unresponsive to stimulation due to the age of the adult testicular cells used in this study (Haider et al., 2007). Alternatively, maximal stimulation was induced by gonadotrophin-like factors in the serum supplement used in the culture medium. Indeed, unresponsiveness of testicular cells to gonadotrophins has been reported before when serum was added to the culture medium (Roulet et al., 2006), while a gonadotrophin-induced increase in hormone production was detected in serum-free systems (Berensztein et al., 2000). Moreover, supplementation of the medium for mouse testicular organ culture with serum alone is sufficient to generate sperm, and, in this setup, lipid-rich albumin plays a critical role (Sato et al., 2011). Unfortunately, many other components of this serum replacement remain unknown. The maintenance of Leydig cells with testis-specific activity was further demonstrated by the production of MCSF, a cytokine important for germ-cell renewal (Martin and Seandel, 2013).

Using three different unambiguous combinations of markers, we found that long-term cultures of scaffold-based and scaffold-free TOs contained early and late spermatogonia. Importantly, throughout the culture period, a proportion of the germ cells stained positive for a marker of proliferation, this being a highly important feature of spermatogonia. However, the number of dividing germ cells appeared to decline with time, which, together with the profile of cytokine secretion, indicates that there is still room for improvement. For instance, certain important inducers of germ-cell renewal, e.g., glial cell-line-derived neurotrophic factor, were not detected by the cytokine array after long-term culture, and, therefore, should perhaps be added to the culture medium (Martin and Seandel, 2013).

The maintenance of the major somatic testicular niche cells with testis-specific functionalities as well as proliferating germ cells documented here represents an important stepping stone for future work on generating haploid cells in TOs. An in vitro model that performs key testicular processes would represent a breakthrough with many valuable



applications. Such a model could help unravel the mechanisms involved in both spermatogenesis and underlying disorders. The 2D models currently available are limited and the results obtained difficult to extrapolate to a tissue (Chapin et al., 2013), while the presently available 3D culture system is suitable only for short-term evaluations (Jørgensen et al., 2015; Roulet et al., 2006). In the clinic, a system enabling in vitro spermatogenesis is the missing link in male fertility preservation and treatment of non-obstructive azoospermia (Gassei and Orwig, 2016). Going further, pluripotent stem cells from men who completely lack germ cells might be combined with TOs to produce artificial gametes more efficiently than what is currently possible (Easley et al., 2012). Finally, the majority of men and women would welcome a male contraceptive to allow their participation in the control of fertility (Kanakis and Goulis, 2016). In this context, and also in the field of reproductive toxicology, an in vitro system for human spermatogenesis could be used to screen candidate drugs and chemicals (Chapin et al., 2013).

EXPERIMENTAL PROCEDURES

See also [Supplemental Experimental Procedures](#).

Donor Testicular Tissue and Formation of TOs

Fragments of DTM were prepared in the manner we described previously (Baert et al., 2015). These fragments were then cryosectioned into 90- μ m discs to obtain testicular scaffolds. Primary testicular cells were isolated from human adult or pubertal testicular tissue by way of two-step enzymatic digestion (Stukenborg et al., 2009). Adult tissue (representing complete spermatogenesis) was donated by six patients undergoing bilateral orchiectomy at the Urology Department, Universitair Ziekenhuis (UZ) Brussel (ethics approval no. 2014/243). All experiments were repeated in triplicate using TOs derived from three different patients. Pubertal testicular tissue was obtained from a 15-year-old who was enrolled in the fertility preservation program at UZ Brussel's Center for Reproductive Medicine (ethics approval no. 2015/V9). This tissue exhibited active spermatogenesis up to meiosis. Because immature tissue is very scarce, it was employed solely to confirm the results obtained with adult tissue. Scaffold-based and scaffold-free TOs were formed by pipetting a drop of medium containing 10^6 cells onto the apical side of a transwell insert containing or lacking a scaffold.

Culture medium (10% [v/v] CTS KnockOut SR XenoFree Medium, $1\times$ GlutaMAX and 1% [v/v] penicillin-streptomycin diluted in KnockOut DMEM; all from Thermo Fisher Scientific) was added to the basolateral compartment of the well with or without (controls) supplementation with human chorionic gonadotrophin (hCG; Pregnyl; Organon) as a luteinizing hormone analog and/or recombinant follicle-stimulating hormone (rFSH; Puregon; Organon), both at physiological concentrations (5 IU/L) (Chada et al., 2003). The cells were cultured for 4 weeks at the gas-liquid interphase at 35°C in a humidified atmosphere containing 5%

CO₂ (Sato et al., 2011), with change of medium every week or when collecting cultured medium for analysis.

Immunofluorescent Staining of Whole Mounts of TOs

To examine the temporal-spatial patterns of the key testicular cell types (Leydig cells, PTMCs, Sertoli cells and spermatogonia [including SSCs]) in TOs, these structures were fixed overnight at 4°C in 4% paraformaldehyde and double immunofluorescent staining of whole mounts was performed. Details of the primary antibodies employed and their targets are provided in [Table S1](#).

Profile of Hormone and Cytokine Secretion

To examine the endocrine functionality of Leydig and Sertoli cells in these TOs, the release of T and InhB, respectively, in response to full gonadotrophic stimulation (rFSH/hCG), stimulation with hCG (-/hCG) or rFSH (rFSH/-) alone, or no stimulation (-/-) was determined at different time points during long-term culture. Concentrations of T (DRG Diagnostics) and InhB (Beckman Coulter) were assayed by employing commercial ELISAs in accordance with the manufacturer's instructions.

Antibody arrays targeting 80 human cytokines (ab133998; Abcam) were used to quantify factors associated with the formation of TOs and to assess major changes in their secretion during culture. To this end, medium collected after short-term (1 week) and long-term (4 weeks) culture was subjected to the antibody array assay in accordance with the manufacturer's instructions.

Statistical Analyses

Statistical analyses were performed by employing GraphPad Prism 6 or IBM Statistics 20 (IBM Corporation) software. Levels (means \pm SDs) of hormones and cytokines were compared by way of two-way ANOVA. These analyses were followed by Bonferroni post hoc tests for correction of multiple comparisons. A p value of <0.05 was considered to be statistically significant.

SUPPLEMENTAL INFORMATION

Supplemental Information includes Supplemental Experimental Procedures, three figures, and two tables and can be found with this article online at <http://dx.doi.org/10.1016/j.stemcr.2016.11.012>.

AUTHORS CONTRIBUTIONS

Y.B., J.D.K., J.-B.S., and E.G. designed the study. Y.B. performed the experiments, the analyses, and interpretation of the data. J.P.A.-L. and J.D.K. obtained and reviewed hormone measurements and secretion profile data, respectively. Y.B., O.S., J.-B.S., and E.G. obtained funding. Y.B. wrote the manuscript and all authors contributed to revision of the paper.

ACKNOWLEDGMENTS

The authors are grateful to Dr. Michiel Martens (Université Libre de Bruxelles) for assistance with confocal imaging and to Dr. Nick Bolton for English language editing. We also wish to thank the Autopsy and Urology Departments at UZ Brussel for the collection of donor material. This study was supported financially by the



Agency for Innovation by Science and Technology (IWT; SB/111245), the Willy Gepts Fund of UZ Brussel (WFWG15-01), a Methusalem (METH3), a travel grant from the Scientific Research Foundation Flanders (FWO; V434114N), FWO-Kom Op Tegen Kanker (KOTK; G.0E39.14N), the Vrije Universiteit Brussel (BAS50), the Swedish Research Council/Finnish Academy of Science (2012-6352), the Emil and Wera Cornell Foundation, the Jeansson Foundation (JS2014-0091), the Swedish Childhood Cancer Foundation (TJ2016-0093), and Sällskapet Barnavård, as well as through the regional agreement on medical training and clinical research (ALF) between Stockholm County Council and Karolinska Institutet. J.P.A.L. was supported by the EU-FP7-PEOPLE-2013-ITN 603568: "Growsperm."

Received: July 20, 2016

Revised: November 25, 2016

Accepted: November 25, 2016

Published: December 22, 2016

REFERENCES

- Baert, Y., Stukenborg, J.-B., Landreh, M., De Kock, J., Jörnvall, H., Söder, O., and Goossens, E. (2015). Derivation and characterization of a cytotocompatible scaffold from human testis. *Hum. Reprod.* *30*, 256–267.
- Berensztein, E., Saraco, N., Belgorosky, A., and Rivarola, M.A. (2000). Enhancement of long-term testosterone secretion and steroidogenic enzyme expression in human Leydig cells by co-culture with human Sertoli cell-enriched preparations. *Eur. J. Endocrinol.* *142*, 481–485.
- Brown, B.N., and Badylak, S.F. (2014). Extracellular matrix as an inductive scaffold for functional tissue reconstruction. *Transl. Res.* *163*, 268–285.
- Chada, M., Průša, R., Bronsky, J., Pechová, M., Kotaška, K., and Lisá, L. (2003). Inhibin B, follicle stimulating hormone, luteinizing hormone, and estradiol and their relationship to the regulation of follicle development in girls during childhood and puberty. *Physiol. Res.* *52*, 341–346.
- Chapin, R.E., Boekelheide, K., Cortvrindt, R., van Duursen, M.B.M., Gant, T., Jegou, B., Marczylo, E., van Pelt, A.M.M., Post, J.N., Roelofs, M.J.E., et al. (2013). Assuring safety without animal testing: the case for the human testis *in vitro*. *Reprod. Toxicol.* *39*, 63–68.
- Cremades, N., Sousa, M., Bernabeu, R., and Barros, A. (2001). Developmental potential of elongating and elongated spermatids obtained after in-vitro maturation of isolated round spermatids. *Hum. Reprod.* *16*, 1938–1944.
- DeFalco, T., Potter, S.J., Williams, A.V., Waller, B., Kan, M.J., and Capel, B. (2015). Macrophages contribute to the spermatogonial niche in the adult testis. *Cell Rep.* *12*, 1107–1119.
- Díez-Torre, A., Silván, U., Moreno, P., Gumucio, J., and Aréchaga, J. (2011). Peritubular myoid cell-derived factors and its potential role in the progression of testicular germ cell tumours. *Int. J. Androl.* *34*, e252–e265.
- Easley, C.A., 4th, Phillips, B.T., McGuire, M.M., Barringer, J.M., Valli, H., Hermann, B.P., Simerly, C.R., Rajkovic, A., Miki, T., Orwig, K.E., and Schatten, G.P. (2012). Direct differentiation of human pluripotent stem cells into haploid spermatogenic cells. *Cell Rep.* *2*, 440–446.
- Gassei, K., and Orwig, K.E. (2016). Experimental methods to preserve male fertility and treat male factor infertility. *Fertil. Steril.* *105*, 256–266.
- Haider, S.G., Servos, G., and Tran, N. (2007). The leydig cell in health and disease. In *Leydig Cell Heal Dis*, A.H. Payne and M.P. Hardy, eds. (Humana Press).
- Jørgensen, a., Nielsen, J.E., Perlman, S., Lundvall, L., Mitchell, R.T., Juul, A., and Rajpert-De Meyts, E. (2015). Ex vivo culture of human fetal gonads: manipulation of meiosis signalling by retinoic acid treatment disrupts testis development. *Hum. Reprod.* *30*, 2351–2363.
- Kanakis, G.A., and Goulis, D.D. (2016). Male contraception: a clinically-oriented review. *Hormones* *14*, 598–614.
- Lee, J.H., Kim, H.J., Kim, H., Lee, S.J., and Gye, M.C. (2006). *In vitro* spermatogenesis by three-dimensional culture of rat testicular cells in collagen gel matrix. *Biomaterials* *27*, 2845–2853.
- Martin, L.A., and Seandel, M. (2013). Propagation of adult SSCs: from mouse to human. *Biomed. Res. Int.* *2013*, 384–734.
- Martinovitch, P.N. (1937). Development *in vitro* of the mammalian gonad. *Nature* *139*, 413.
- Mruk, D.D., and Cheng, C.Y. (2004). Sertoli-Sertoli and Sertoli-germ cell interactions and their significance in germ cell movement in the seminiferous epithelium during spermatogenesis. *Endocr. Rev.* *25*, 747–806.
- Reda, A., Hou, M., Landreh, L., Kjartansdóttir, K.R., Svechnikov, K., Söder, O., and Stukenborg, J.-B. (2014). *In vitro* spermatogenesis – optimal culture conditions for testicular cell survival, germ cell differentiation, and steroidogenesis in rats. *Front. Endocrinol.* *5*, 1–11.
- Reda, A., Hou, M., Winton, T.R., Chapin, R.E., Söder, O., and Stukenborg, J.-B. (2016). In vitro differentiation of rat spermatogonia into round spermatids in tissue culture. *Mol. Hum. Reprod.* *22*, 601–622.
- Roulet, V., Denis, H., Staub, C., Le Tortorec, A., Delaleu, B., Satie, A.P., Patard, J.J., Jégou, B., and Dejucq-Rainsford, N. (2006). Human testis in organotypic culture: application for basic or clinical research. *Hum. Reprod.* *21*, 1564–1575.
- Sato, T., Katagiri, K., Gohbara, A., Inoue, K., Ogonuki, N., Ogura, A., Kubota, Y., and Ogawa, T. (2011). *In vitro* production of functional sperm in cultured neonatal mouse testes. *Nature* *471*, 504–507.
- Schlatt, S., Weinbauer, G.F., Arslan, M., and Nieschlag, E. (1993). Appearance of alpha-smooth muscle actin in peritubular cells of monkey testes is induced by androgens, modulated by follicle-stimulating hormone, and maintained after hormonal withdrawal. *J. Androl.* *14*, 340–350.
- Siu, M.K.Y., and Cheng, C.Y. (2004). Dynamic cross-talk between cells and the extracellular matrix in the testis. *Bioessays* *26*, 978–992.
- Stukenborg, J.-B., Schlatt, S., Simoni, M., Yeung, C.-H., Elhija, M.A., Luetjens, C.M., Huleihel, M., and Wistuba, J. (2009). New horizons for *in vitro* spermatogenesis? An update on novel



three-dimensional culture systems as tools for meiotic and post-meiotic differentiation of testicular germ cells. *Mol. Hum. Reprod.* *15*, 521–529.

Valentin, J.E., Stewart-Akers, A.M., Gilbert, T.W., and Badylak, S.F. (2009). Macrophage participation in the degradation and remodeling of extracellular matrix scaffolds. *Tissue Eng. Part A.* *15*, 1687–1694.

Yin, X., Mead, B.E., Safaei, H., Langer, R., Karp, J.M., and Levy, O. (2016). Engineering stem cell organoids. *Cell Stem Cell* *18*, 25–38.

Yokonishi, T., Sato, T., Katagiri, K., Komeya, M., Kubota, Y., and Ogawa, T. (2013). *In vitro* reconstruction of mouse seminiferous tubules supporting germ cell differentiation. *Biol. Reprod.* *89*, 1–6.